SYNTHESIS OF NANOCELLULOSE AS MECHANICAL REINFORCEMENT OF THERMOPLASTIC STARCH

SÍNTESIS DE NANOCELULOSA COMO REFUERZO MECÁNICO DE ALMIDÓN TERMOPLÁSTICO

Antony A. Neciosup-Puican[1*], José A. Castañeda-Vía[2], Carlos V. Landauro[1,3], Justiniano Quispe-Marcatoma[1,3], Ilanit Samolski[4] and Gretty K. Villena[4]

[1] Facultad de Ciencias Físicas, Universidad Nacional Mayor de San Marcos, Lima, Perú.
[2] Escuela de Posgrado "Víctor Alzamora Castro", Universidad Peruana Cayetano Heredia, Lima, Perú.
[3] Centro de Investigaciones, Tecnológicas, Biomédicas y Medioambientales (CITBM), Callao, Perú.
[4] Laboratorio de Micología y Biotecnología "Marcel Gutiérrez-Correa", Universidad Nacional Agraria La Molina, Lima, Perú.

(Recibido: 07/2022. Aceptado: 04/2023)

Abstract

Nanocellulose was successfully synthetized from microcrystalline cellulose by an acid hydrolysis process. The sample characterization was performed employing X-ray diffraction, zeta potential and confocal Raman microscopy. Nanocellulose-reinforced thermoplastic starch (TPS) composites were prepared by solution casting method, in which a small concentration of nanocellulose improved the elastic modulus of TPS. This property was calculated using the atomic force microscopy nanoindentation method. We conclude that nanocellulose is a good mechanical reinforcement for composites from commercial sources as starch.

Keywords: thermoplastic, nanocellulose, mechanical properties.

* antony.neciosup@unmsm.edu.pe doi: https://doi.org./10.15446/mo.n67.103549

Resumen

Se sintetizó exitosamente nanocelulosa a partir de celulosa microcristalina mediante un proceso de hidrólisis ácida. La caracterización de la muestra se realizó mediante difracción de rayos X, potencial zeta y microscopía Raman confocal. Se prepararon compuestos de almidón termoplástico (TPS, por sus siglas en inglés) reforzados con nanocelulosa mediante el método "casting solution", en el que una pequeña concentración de nanocelulosa mejoró el módulo de elasticidad del TPS. Esta propiedad se calculó mediante el método de nanoindentación por microscopía de fuerza atómica. Llegamos a la conclusión de que la nanocelulosa es un buen refuerzo mecánico para los compuestos de fuentes comerciales como el almidón.

Palabras clave: termoplástico, nanocelulosa, propiedades mecánicas.

Introduction

Basic packaging materials, such as paper, plastic, glass, and a combination of materials of various chemical and physical structures, are used to fulfil functions and requirements that packaged foods require, depending on their type. Among them, plastic materials have been widely used since the middle of the 20th century causing a serious environmental problem because they do not easily degrade in the environment after use [1] [2]. Thus, there is a growing demand for biodegradable packaging materials from renewable sources as an alternative to synthetic plastic packaging materials. The ideal biodegradable packaging materials are obtained from renewable biological resources, generally natural polymers (biopolymers) [3].

Among all biopolymers, starch is one of the most promising biocompatible and biodegradable materials, which has received attention due to its advantages such as low cost, wide availability, and full compostability without the formation of toxic residues [4]. However, starch alone is not a true plastic, it must be processed in the presence of heat and mechanical treatment together with a plasticizer, in which the starch granules undergo an alteration

that leads to a homogeneous melt that is known as thermoplastic starch (TPS) [5]. However, these materials have not yet been widely introduced as consumer goods, due to some major drawbacks; basically, their low mechanical properties [3].

On other hand, cellulose is the most abundant organic compound on earth and is found in the plant cell wall. The natural nano-reinforcement derived from cellulose, called nanocellulose, can be obtained using controlled sulfuric acid hydrolysis. In acid hydrolysis, the amorphous portion of cellulose readily hydrolyzes under strong acid conditions leaving individual crystals [5]. One of the main advantages of the reinforcing cellulose material in the starch matrix is the presence of a similar polysaccharide structure that could benefit from a better matrix/filler interaction. Considering this context, the present study reports the preparation of nanocomposite thermoplastic starch reinforced with nanocellulose, evaluating its physicochemical properties for its potential use in the food industry.

1. Experimental procedure

1.1. Materials

Corn starch (Duryea Maizena, Unilever, Peru) was purchased in a small traditional market in Lima. Microcrystalline cellulose (CAS N° 9004-34-6) and sulfuric acid (CAS N° 7664-93-9) were purchased from Sigma-Aldrich.

1.2. Preparation of Nanocellulose

Cellulose nanocrystals were synthesized from microcrystalline cellulose using the acid hydrolysis method [6]. In this process, 5 g of microcrystalline cellulose with 45 mL sulfuric acid (H_2SO_4, 64 wt. %) were mixed at 250 rpm and kept at 45 °C for 120 min. Subsequently, they were washed by centrifugation with distilled water for 15 min at 5000 rpm. After centrifugation, the supernatant was removed and replaced by distilled water. This process was repeated three times until the supernatant reached a pH of 1.0.

The last wash was placed in a dialyzer with distilled water until the wash water maintained a constant pH of 7.0. The resulting suspension was stored at 4 °C until further analysis.

1.3. Preparation of Thermoplastic Starch (TPS)

For the preparation of the TPS, a chemical casting or casting process was followed [7] 5 g of starch powder with 100 mL distilled water were mixed at 98 °C with continuous stirring for 10 min. To avoid air bubbles, the solution was passed by ultrasound over 10 min. After that, 25 g of the gelatinized suspension were spread into a glass Petri (10 cm diameter) and dried at 45 °C for 48 h in a dry oven. For the preparation of nanocomposites, 10 wt. % nanocellulose in suspension (0.5 g), relative to the starch mass was added. All the samples were stored in a closed desiccator with concentrated sulfuric acid at 25 °C for complete drying.

1.4. X-ray Diffraction (XRD)

The structural properties of the nanocellulose and microcrystalline cellulose were analyzed by X- ray diffraction technique using a D8 Focus diffractometer (Bruker AXS, Karlsruhe, Germany), operated at 40 kV and 40 mA with Cu-Kα radiation ($\lambda = 1.506$ $\mathring{A}$). The crystallinity index and the crystallite size were determined by the Segal method and the Scherer equation, respectively.

1.5. Zeta potential

The stability of the nanocellulose in suspension was analyzed by successive measurements using a NICOMP Nano Z3000 System (Entegris Inc., Massachusetts, USA), which provides the distribution curve of zeta potential.

1.6. Confocal Raman Microscopy (CRM)

The chemical composition of the nanocellulose and microcrystalline cellulose were analyzed by Raman spectroscopy using a confocal Raman microscope alpha300 RA (WITec GmbH, Ulm, Germany).

The measurements were made by line mode using 50 points along 140 µm, taking 20 measurements of 0.5 seconds at each point. The objective used was a 20x Zeiss EC Epiplan, and the excitation source was a Nd:YAG laser with a wavelength of 784 nm and a power of 50 mW.

1.7. Mechanical Testing

The mechanical properties of the TPS with and without nanocellulose were measured using an atomic force microscope alpha300 RA (WITec GmbH, Ulm, Germany). Nanoindentation measurements were performed in contact mode, considering five indentations per sample with a depth of 100 nm and a setpoint of 0.5 V. The calculated elastic modulus values were analyzed using the non-parametric Kruskal-Wallis test to find significant differences between both samples. Then, the Bonferroni test was used to compare the study samples using the STATA 16 software (StataCorp LLC, Texas, USA) with a significance level of 5 % ($p<0.05$).

2. Results and Discussions

2.1. Crystalline Structure by XRD

X-ray diffractograms of microcrystalline cellulose and nanocellulose are shown in Figure 1, where four peaks were observed for both samples (2θ = 14.7°, 16.5°, 22.5° and 34.7°). These peaks are characteristic of crystalline polymorph Iα of cellulose (spatial group P1, triclinic system) since it does not present a doublet in the main peak at 2θ = 22.5° [8, 9]. This type of polymorph is characterized by the fact that the parallel chains are strongly linked by intermolecular hydrogen bonds [10]. The peaks at $2\theta = 14.7°$ and 16.3° correspond to the (110) and (1$\bar{1}$0) planes, 2θ = 22.5° for the (200) plane, and the peak at 2θ = 34.7° corresponds to the (004) plane [11].

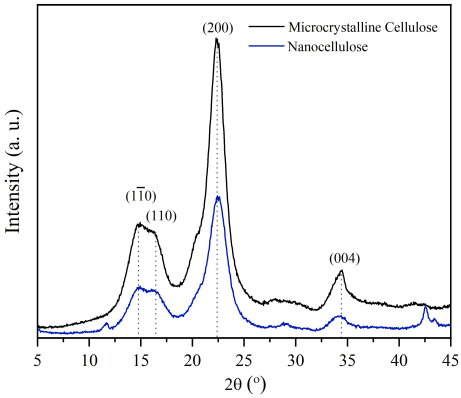

FIGURE 1. *X-ray diffraction pattern of microcrystalline cellulose and nanocellulose.*

Segal et al. [12] suggested estimation of the crystallinity index by:

$$I_{Cr} = 100\frac{I_{hkl} - I_{am}}{I_{hkl}} \tag{1}$$

Where I_{cr} is the crystallinity index, I_{am} is the amorphous zone diffraction intensity of 2θ equal to 18°, and I_{hkl} is the crystalline zone diffraction intensity on the (200) lattice plane. On the other hand, the crystallite size (D) was calculated using the Scherrer equation:

$$D = \frac{0.9\lambda}{\beta cos\theta} \tag{2}$$

Where D is the crystal dimension upright to the diffracting planes, $\lambda = 1.506\ \mathring{A}$, β is the full width at half-maximum of diffraction peak and θ is the corresponding Bragg angle [13].

Crystallinity index values and the crystallite size are shown in Table 1. In this study, the crystallinity index of the prepared nanocellulose is slightly higher than that of microcrystalline cellulose under hydrolysis conditions. It was expected that the nanocellulose presents a significantly higher crystallinity index than that of microcrystalline cellulose, but it did not occur in our samples. These results indicate that during the production of nanocellulose, the hydrolysis reaction not only removed the

amorphous region of cellulose fibrils but also partly destroyed their crystalline region. Additionally, the crystallite size of the nanocellulose was 4.2 nm, in agreement with the work of Jiang and Hsieh, that explain this effect mainly by the narrowing of the crystallite size distribution with the acid hydrolysis [14].

Sample	$\mathbf{I}_{Cr}$ **(%)**	**D (nm)**	**FWHM (cm^{-1})**
Microcrystalline cellulose	85.45	3.7	22.3
Nanocellulose	86.44	4.2	10.8

TABLE 1. *Crystallinity index (I_{Cr}), crystallite size (D) and full width at half maximum of main Raman peak (FWHM) of each type of cellulose samples.*

2.2. Zeta Potential Measurements

The stability of nanocellulose was determined by zeta potential, which evaluates the presence of surface charges. Figure 2 shows the nanocellulose sample in suspension, which has a zeta potential of -39.85 mV (Figure 3). This negative value is ascribed to the insertion of charged sulphate ester groups onto the surface of the nanocellulose, induced by the sulfuric acid treatment, which indicates that the hydrolysis conditions used led to a colloidal dispersion in water electrostatically stabilized by repulsive forces. According to Khouri et al., nanocellulose agglomeration occurs if the value of the zeta potential is within the range of -15 to 15 mV [15]. The nanocellulose particles do not have enough charge to repel each other within this range, so they form agglomerates. The same authors also discussed that a stable suspension of nanocellulose should have a zeta potential value less than -30 mV or greater than 30 mV.

2.3. Chemical Composition by CRM

The chemical composition of nanocellulose was determined by Raman spectroscopy. According to Landry et al., in the low-frequency region, from 250 cm^{-1} to 550 cm^{-1}, the bands are

FIGURE 2. *Nanocellulose sample after acid hydrolysis process.*

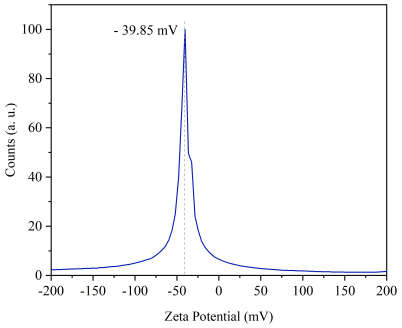

FIGURE 3. *Zeta potential distribution of nanocellulose.*

attributed to the bending of the skeletal bonds corresponding to $C-C-C$, $C-O-C$, $O-C-C$ and $O-C-O$ of internal coordination [16]. These bonds are related to the internal structure of the nanocellulose, which is based on polysaccharide rings and OH groups, and they can react or interact with other functional groups. On the other hand, the region from 950 cm^{-1} to 1180 cm^{-1} represents mainly $C-C$ and $C-O$ bonds in stretching motions and finally the region from 1180 cm^{-1} to 1500 cm^{-1} presents some medium-intensity signals from the bands representing $H-C-C, H-C-O, H-C-H$, and $H-O-C$ in vibrational bending mode [16]. According to Agarwal et al., the intensity and width of the band at 380 cm^{-1} are related to the degree of crystallinity and they showed that the degree of crystallinity is greater when the intensity of this band is larger and sharper [17]. Figure 4 shows that the band at 380 cm^{-1} for nanocellulose is more

intense than that for microcrystalline cellulose, then it is possible to say that material with greater crystallinity was effectively obtained (Table 1).

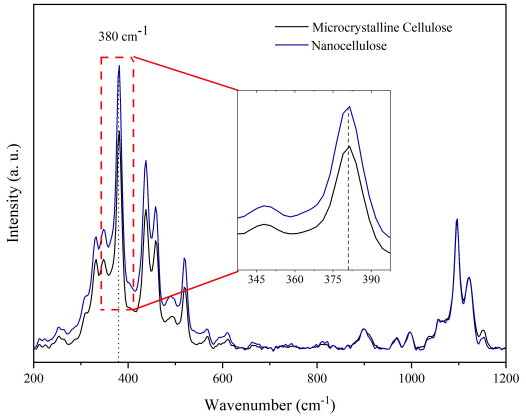

FIGURE 4. *Raman spectra of nanocellulose and microcrystalline cellulose.*

2.4. Mechanical Properties of TPS Nanocomposites

The mechanical properties of TPS samples were analyzed with the Doerner and Nix method, in which a pyramidal-shaped indenter with a triangular base is assumed [18]. The analysis proposes that the plastic displacement, hp, which is the depth of deformation at which the indenter and sample remain in contact, can be extracted from the intersection of the tangent of the discharge curve (S) with the abscissa axis at the point of maximum load (P), as follows:

$$S = 2\left(\frac{A_c}{\pi}\right)^{\frac{1}{2}} E_r \tag{3}$$

Where $A_c = 24.5hp^2$ is the projected contact area on the surface of the sample, and E_r is the reduced elastic modulus. The elastic modulus of the material under study, E, is related to the reduced modulus E_r as follows:

$$\frac{1}{E_r} = \frac{1-\upsilon^2}{E} + \frac{1-\upsilon_0^2}{E_0} \tag{4}$$

Where υ, E and υ_0, E_0 correspond to the Poisson ratio and elastic modulus of the sample and the indenter, respectively. The indenter is normally several orders of magnitude larger than that of polymeric materials, so the second term can be considered negligible.

The elastic modulus is therefore calculated as:

$$E = E_r(1-\upsilon^2) = \frac{1}{2h_p} S \left(\frac{\pi}{24.5}\right)^{\frac{1}{2}} \left(1-\upsilon^2\right) \tag{5}$$

where h_p and S are extracted from the experimental data.

For the calculation of the mechanical properties of thermoplastics, with and without nanocellulose, the materials were considered incompressible ($\upsilon = 0.5$). Thus, the equation (5) is as follows:

$$E = \frac{1}{2h_p} S \left(\frac{\pi}{24.5}\right)^{\frac{1}{2}} (0.75) \tag{6}$$

Figure 5 shows the comparison of the elastic modulus values obtained by nanoindentation, without and with 10 wt. % nanocellulose reinforcement. TPS without nanocellulose had an elastic modulus of 0.23 ± 0.03 GPa. Lendvai et al. showed similar values (0.30 GPa) using a universal testing machine [19]. Also, using the same technique, Tabassi et al. showed that the modulus of elasticity is 0.237 GPa [20], which agrees with that calculated using nanoindentation by the atomic force microscopy technique. On the other hand, TPS with 10 wt. % nanocellulose reinforcement had an elastic modulus of 1.04 ± 0.3 GPa, while Tabassi et al. [20], with 3 wt. % of nanocellulose reported an elastic modulus of 1.29 GPa. The values obtained were statistically different values with a significance value of $p<0.05$. Therefore, according to the proposed model, it can be observed that small amounts of nanocellulose synthesized under hydrolysis conditions improve the elastic modulus of TPS.

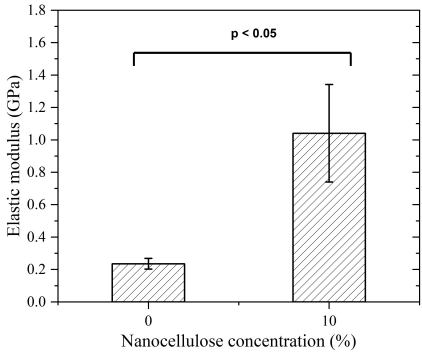

FIGURE 5. *Elastic modulus of TPS without reinforcement and with 10 wt. % nanocellulose reinforcement.*

2.5. Conclusions

Nanocellulose can be prepared under the conditions of acid hydrolysis. The physicochemical characterization of these samples verified the presence of stable nanocellulose. This material provides a significant change in the elastic modulus of the starch thermoplastic, which was calculated using nanoindentation by the atomic force microscopy technique. Finally, it is worth mentioning that the procedure followed in the present work allows to prepare a TPS nanocomposite with enhanced mechanical properties. Besides, it opens the possibility to incorporate another material in the composites to obtain new properties. For instance, by incorporating Ag nanoparticles, the composites could exhibit antibacterial properties. Such work is currently underway.

2.6. Acknowledgements

The authors are grateful to Dr. Verónica Carranza from the Faculty of Chemistry and Chemical Engineering of the Universidad Nacional Mayor de San Marcos (UNMSM) for the zeta potential measurements. This work was supported by Concytec through its executing unit ProCiencia [grant numbers 083-2018-FONDECYT-BM-IADT-AV, 08-2018-FONDECYT-BM], and the Excellence Centers Program.

References

[1] J.-W. Rhim, H.-M. Park, and C.-S. Ha, Prog. Polym. Sci. **38**, 1629 (2013).

[2] P. Suppakul, J. Miltz, K. Sonneveld, and S. Bigger, J. Food Sci. **68**, 408 (2006).

[3] R. Zhao, P. Torley, and P. Halley, J Mater Sci. **43**, 3058 (2008).

[4] A. Mathew and A. Dufresne, Biomacromolecules **3**, 609 (2002).

[5] M. Agustin and et al, J. Reinf. Plast. Comp. **33**, 2205 (2014).

[6] Y. Zhou, S. Fu, L. Zheng, and H. Zhan, Express Polym. Lett. **6**, 794 (2012).

[7] A. Jiménez and et al, Food Bioprocess Technol. **5**, 2058.

[8] K. Dome, E. Podgorbunskikh, A. Bychkov, and O. Lomovsky, Polym. **12** (2020).

[9] R. Li and et al, Carbohydr. Polym. **76**, 94 (2009).

[10] A. Walther, J. Timonen, I. Díez, A. Laukkanen, and O. Ikkala, Adv. Mater. **23**, 2924 (2011).

[11] A. Thygesen, J. Oddershede, H. Lilholt, A. Thomsen, and K. Stahl, Cellulose **12**, 563 (2005).

[12] L. Segal, J. Creely, A. Martin, and C. Conrad, Text. Res. J. **29**, 786 (1959).

[13] J. Revol, A. Dietrich, and D. Goring, Can. J. Chem. **65**, 1724 (1987).

[14] F. Jiang and Y.-L. Hsieh, Carbohydr. Polym. **95**, 32 (2013).

[15] S. Khouri, *Experimental Characterization and Theoretical Calculations of Responsive Polymeric Systems (Master thesis)* (Ontario, Department of Chemical Engineering, Faculty of Engineering, Universidad of Waterloo, 2010) pp. 63–65.

[16] V. Landry, A. Alemdar, and P. Blanchet, For. Prod. J. **61**, 104 (2011).

[17] U. Agarwal, R. Reiner, and S. Ralph, Cellulose **17**, 721 (2010).

[18] M. Doerner and W. Nix, J. Mater. Res. **1**, 601 (1986).

[19] L. Lendvai and et al, J. Appl. Polym. Sci. **133**, 601 (2016).

[20] N. Tabassi, M. Moghbeli, and I. Ghasemi, Iran. Polym. J. **25**, 45 (2016).